Journal of Molecular Catalysis B: Enzymatic 84 (2012) 27–34

Contents lists available at SciVerse ScienceDirect

Journal of Molecular Catalysis B: Enzymatic

journal homepage: www.elsevier.com/locate/molcatb

Comparative investigations on thermostable pyrimidine nucleoside phosphorylases from *Geobacillus thermoglucosidasius* and *Thermus thermophilus*

Kathleen Szeker[a,*], Xinrui Zhou[a], Thomas Schwab[b], Ana Casanueva[c], Don Cowan[c], Igor A. Mikhailopulo[d], Peter Neubauer[a]

[a] Department of Bioprocess Engineering, Institute of Biotechnology, Technische Universität Berlin, Ackerstr. 71-76, ACK24, 13355 Berlin, Germany
[b] Institute of Biophysics and Physical Biochemistry, University of Regensburg, Universitätsstrasse 31, 93053 Regensburg, Germany
[c] Institute for Microbial Biotechnology and Metagenomics, University of the Western Cape, Private Bag X17, Bellville 7535, Cape Town, South Africa
[d] Institute of Bioorganic Chemistry, National Academy of Sciences of Belarus, Acad. Kuprevicha 5/2, 220141 Minsk, Belarus

ARTICLE INFO

Article history:
Available online 25 February 2012

Keywords:
Biocatalysis
Thermostable pyrimidine nucleoside phosphorylase
Pyrimidine nucleoside
2′-Deoxyfluoro nucleosides
Thermus thermophilus
Geobacillus thermoglucosidasius

ABSTRACT

The recombinant expression and biocatalytic characterization of two thermostable pyrimidine nucleoside phosphorylases (PyNP), isolated from *Geobacillus thermoglucosidasius* (Gt) and *Thermus thermophilus* (Tt) is described. Both enzymes are highly thermostable (half life of GtPyNP is 1.6 h at 70 °C, half life of TtPyNP is >24 h at 80 °C). Kinetic parameters for the phosphorolysis of natural substrates were determined for GtPyNP at 60 °C (K_m for uridine 2.3 mM, K_m for thymidine 1.3 mM) and TtPyNP at 80 °C (K_m for uridine 0.15 mM, K_m for thymidine 0.43 mM). The k_{cat} values for uridine are almost identical for both enzymes (ca. 277 s^{-1}), while the k_{cat} value for thymidine is about 8 times higher for TtPyNP than for GtPyNP (679 s^{-1} vs. 83 s^{-1}).

Both enzymes were tested towards the ability to catalyze the phosphorolytic cleavage of 2′-fluorosubstituted pyrimidine nucleosides – a prerequisite for the efficient synthesis of a number of relevant purine nucleoside analogues. GtPyNP showed poor activity towards 2′-deoxy-2′-fluorouridine ($dUrd_{2'F}$; 0.4% substrate conversion after 30 min), and the phosphorolysis of the epimeric counterpart 1-(2-deoxy-2-fluoro-β-D-arabinofuranosyl)uracil ($dUrd^{2'F}$) could not be detected at all. By contrast, TtPyNP showed dramatically higher conversion rates (15.6% and 1.6% conversion in 30 min of both substrates, respectively). The amount of converted pyrimidine nucleosides increased significantly with time. After 17 h 65% of $dUrd_{2'F}$ and 46% of $dUrd^{2'F}$ was phosphorolytically cleaved.

Our results demonstrate the potential of TtPyNP as a biocatalyst in transglycosylation reactions aiming at the production of 2′-fluorosubstituted purine nucleosides that are highly bioactive but hardly accessible by chemical methods.

1. Introduction

Pyrimidine nucleoside phosphorylases (PyNP; EC 2.4.2.2) are homodimeric enzymes that are involved in the nucleotide salvage pathway of some lower organisms [1–3]. In the presence of phosphate ions, PyNP catalyzes the reversible phosphorolytic cleavage of the glycosidic bond of pyrimidine nucleosides or closely related derivatives thereof according to the following general reaction scheme (Scheme 1).

Structurally, PyNP is closely related to human thymidine phosphorylases (TP; EC 2.4.2.4) – an angiogenic enzyme that was found to be identical to the platelet-derived endothelial cell growth factor in humans [4,5]. Together, TP and PyNP form the nucleoside phosphorylase-II family, which share a common two-domain subunit fold and a high level of sequence identity [3]. Despite the similarity of the reaction catalyzed, uridine phosphorylase (UP; EC 2.4.2.3) belongs to the phosphorylase-I family with distinct structural characteristics. From the catalytical point of view, TP is distinguished from UP due to its high specificity for the 2′-deoxy-D-ribofuranose moiety of pyrimidine nucleosides [3]. By contrast, PyNP does not discriminate between uridine (**1**) and thymidine (**2**) and accepts both compounds as natural substrates [6].

This rather broad substrate specificity makes PyNP a versatile biocatalyst suitable for certain synthetic applications, e.g. for the

Abbreviations: PyNP, pyrimidine nucleoside phosphorylase; PNP, purine nucleoside phosphorylase; NP, nucleoside phosphorylase; TP, thymidine phosphorylase; UP, uridine phosphorylase; Tt, *Thermus thermophilus*; Gt, *Geobacillus thermoglucosidasius*; $dUrd_{2'F}$, 2′-deoxy-2′-fluorouridine; $dUrd^{2'F}$, 1-(2-deoxy-2-fluoro-β-D-arabinofuranosyl)uracil.

* Corresponding author. Tel.: +49 30 314 72521; fax: +49 30 314 27577.
E-mail addresses: k.szeker@mailbox.tu-berlin.de (K. Szeker), xinrui.zhou@gmail.com (X. Zhou), thomas.schwab@biologie.uni-regensburg.de (T. Schwab), acasanueva@uwc.ac.za (A. Casanueva), dcowan@uwc.ac.za (D. Cowan), igormikh@iboch.bas-net.by (I.A. Mikhailopulo), peter.neubauer@tu-berlin.de (P. Neubauer).

1381-1177/$ – see front matter © 2012 Elsevier B.V. All rights reserved.
doi:10.1016/j.molcatb.2012.02.006

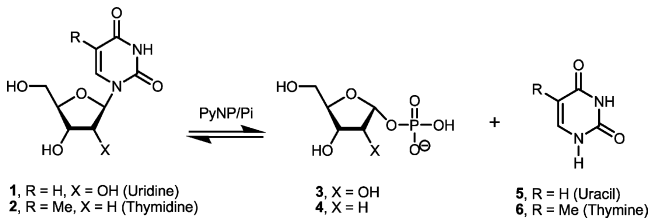

Scheme 1.

enzymatic synthesis of nucleosides. Of particular interest is the synthesis of modified nucleosides, that can be used as pharmaceutical agents for the treatment of viral infections and cancer, as well as in molecular biological techniques and diagnostics [7–10]. For their synthesis, efficient chemo-enzymatic approaches have been developed, among them the enzymatic transglycosylation of chemically modified nucleosides [11]. Scheme 2 illustrates the enzymatic synthesis of modified purine nucleosides as an example: by the concerted action of a PyNP and a purine nucleoside phosphorylase (PNP; EC 2.4.2.1), a pentofuranosyl moiety is transferred from a pyrimidine nucleoside that serves as pentofuranosyl donor to a heterocyclic purine base that serves as pentofuranosyl acceptor. It is obvious that the lack of enzymes with broad substrate specificities is limiting the application spectrum of this strategy. In addition, the efficiency of such processes, when run at high temperatures, is often reduced due to the thermal lability of the biocatalysts.

The search for enzymes with improved properties is hence of prime importance in this field of research and prompted us to investigate biocatalytical characteristics of novel nucleoside phosphorylases. In contrast to PNPs that have been extensively studied from a multitude of mesophilic and thermophilic (micro) organisms [12–15], PyNPs have been hardly studied in detail. Only few examples can be found in the scientific literature: PyNP from *Bacillus subtilis* [16], *Geobacillus stearothermophilus* [1,2,6] and from *T. thermophilus* [17]. With respect to practical use as biocatalyst, only the *G. stearothermophilus* enzyme has been described [18].

In the present study, we report on the recombinant expression and characterization of two additional thermostable PyNPs, derived from *G. thermoglucosidasius* 11955 (GtPyNP) and *T. thermophilus* HB27 (TtPyNP), respectively. Albeit the expression and crystallization of PyNP from *T. thermophilus* HB8 has been reported [17], information about the biocatalytic characterization is not available. Here, we investigate thermal characteristics and kinetic parameters as well as the ability to phosphorolyze 2′-fluorosubstituted pyrimidine nucleosides, *viz.*, 2′-deoxy-2′-fluorouridine ($dUrd_{2'F}$) and 1-(2-deoxy-2-fluoro-β-D-arabinofuranosyl)uracil ($dUrd^{2'F}$) (Scheme 2), which are of special interest, as sugar donors, for purine nucleoside synthesis. Our data reveal striking differences of the conversion rates depending on the substrate analogue and the biocatalyst applied.

2. Experimental

2.1. Molecular biology

G. thermoglucosidasius 11955 was grown for 1.5 days at 52 °C in Luria Broth (10 g l^{-1} tryptone, 5 g l^{-1} yeast extract, 10 g l^{-1} NaCl, pH 7.0), whereas *T. thermophilus* HB27 was grown as previously described [19]. Genomic DNA of both strains was isolated using standard protocols [20]. The genes coding for PyNP in *G. thermoglucosidasius* (GenBank accession no. ZP_06809030) and *T. thermophilus* (GenBank accession number AAS81754.1) were amplified using Pfu DNA polymerase (Fermentas, Lithuania). The following primer pair was used for the isolation of the PyNP gene from the *G. thermoglucosidasius* genome: 5′ ACTAGGGATCCATGGTCGATTTAATTGCGA 3′ (*Bam*HI site underlined) and 5′ AGCATGCGGCCGCTTATGAAATGGTTTCGTATATA 3′ (*Not*I site underlined). The primer pair used for the *T. thermophilus* gene was: 5′ ACTAGGGATCCAACCCCGTGGTCTTCATC 3′ (*Bam*HI

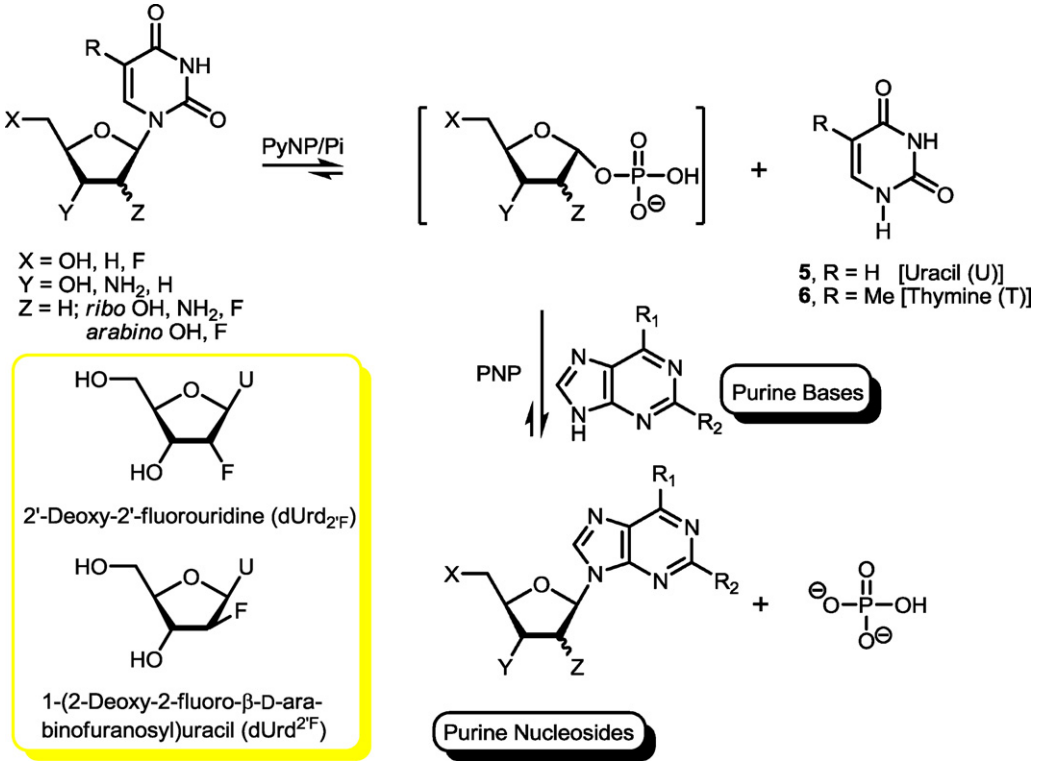

Scheme 2.

site underlined) and 5′ AGCATGCGGCCGCCTAGATGGCCTCCAGGA 3′ (*Not*I site underlined). The PyNP encoding genes were cloned via *Bam*HI/*Not*I digestion (FastDigest restriction endonucleases, Fermentas, Lithuania) and subsequent ligation (T4 DNA Ligase, Roche) into a derivative of the expression vector pCTUT7 [21]. This vector is characterized by an IPTG inducible *lac* promoter derivative and a pBR322 origin of replication. We have modified this vector before by substituting the chloramphenicol resistance cassette by the plasmid stabilizing *parB* locus [22] and an ampicillin resistance cassette. In addition we introduced a sequence encoding a hexahistidine tag connected to the 5′-end of target gene's transcript. The resulting expression vectors were transformed into the *Escherichia coli* BL21 strain (Novagen).

2.2. Bioinformatics and homology modeling

Amino acid sequence identities were assessed with the protein basic local alignment tool (BLAST) [23] of the NCBI web server. For multiple sequence alignments the ClustalW2 program from the EBI web server was used [24]. Three-dimensional protein structures of the target proteins were built by homology modeling using the Swiss-model workspace [25]. These 3D models were superposed and visualized with the CCP 4 mg molecular-graphics software [26].

2.3. Overexpression in E. coli

Recombinant *E. coli* strains were cultivated in terrific broth (TB) medium [27] or EnPresso® medium (BioSilta, Finland) using Ultra Yield Flasks™ and AirOTop™ seals (Thomson Instrument Company, USA). Recombinant protein expression was induced by addition of IPTG to a final concentration of 100 μM, after 2.5 h cultivation time (TB medium) or after overnight cultivation (EnPresso medium). Cells were harvested (centrifugation at 16,000 × *g*, 5 min, 4 °C) 3 h after induction (TB medium) or 24 h after induction (EnPresso medium) and stored at −20 °C.

2.4. Cell disruption and purification

Cell pellets were re-suspended in NPI-10 binding buffer (50 mM NaH_2PO_4, 300 mM NaCl, 10 mM imidazole, pH 8.0) at 5 ml/g wet weight. This cell suspension was sonicated on ice using a UP200S sonicator (Hielscher Ultrasonics GmbH). The sonication was performed twice with 30% power input for 3 min in 30 s intervals using a sonotrode of 7 mm in diameter.

Cell lysates were centrifuged (20,000 × *g*, 15 min, 4 °C) to separate soluble from insoluble fraction. The soluble portion of the cell lysate was heated for 15 min at 60 °C (GtPyNP) or 80 °C (TtPyNP). Coagulated proteins were removed by centrifugation (20,000 × *g*, 15 min, 4 °C). The target proteins were further purified by immobilized metal ion affinity chromatography using a 5 ml Ni-NTA Superflow cartridge (Qiagen), subsequently the excess of salt and imidazole was removed by the use of a HiPrep 26/10 Desalting column (GE Healthcare). The purified protein solution was aliquoted, rapidly frozen in liquid nitrogen and stored at −80 °C.

2.5. Protein analytics

The protein concentration of the purified protein solution was determined by measuring the absorption at 280 nm (Nanodrop, Thermo Scientific). The absorption coefficients were theoretically calculated from the amino acid sequence (Vector NTI software, Invitrogen) and were 0.42 AU (GtPyNP) and 0.56 AU (TtPyNP) for a solution of 1 mg ml^{-1}.

The molecular weight marker for SDS-PAGE analysis was purchased from Fermentas (Lithuania).

Protein unfolding: Thermal denaturation of 10 μM purified TtPyNP protein dissolved in potassium phosphate (50 mM, pH 7.5) was monitored with a Jasco J-815 circular dichroism (CD) spectrometer in a 0.1 cm cuvette by following the loss of ellipticity at 220 nm. Unfolding was induced by raising the temperature in 0.1 °C increments at a ramp rate of 1 °C min^{-1} with a Peltier-effect temperature controller. The measured ellipticity was normalized, and the apparent melting temperature (T_M^{app}) was determined. DSC experiments were performed with 43 μM TtPyNP protein dissolved in potassium phosphate (50 mM, pH 7.5) by heating the samples in a CSC 5100 Nano differential scanning calorimeter with a scan rate of 1 °C min^{-1}. The DSC data were analyzed with the program CpCalc (version 2.1, Calorimetry Sciences Corporation, 1995) to determine T_M^{app} at which half of the protein is unfolded. The irreversibility of thermal denaturation precluded thermodynamic analysis of the CD and DSC unfolding traces.

2.6. Activity assay

If not otherwise stated the activity assay was performed in 50 mM potassium phosphate buffer, pH 7.0 containing 1 mM of uridine as substrate. After 2 min of pre-heating, 1–2 μl of diluted enzyme was added per 100 μl of reaction mixture. Samples were withdrawn after defined time intervals and the reaction was immediately stopped by adding 1 volume of reaction mixture to ½ volume of 10% trichloroacetic acid. Precipitated proteins were removed by centrifugation (20,000 × *g*, 15 min) and the samples were stored at −20 °C for later analysis by HPLC.

From the HPLC results the concentration of residual pyrimidine nucleoside (substrate) and liberated pyrimidine base (product of the phosphorolytic cleavage) was retrieved. The substrate conversion was calculated with the following formula:

$$\text{Conversion}\,(\%) = \frac{\text{base}}{\text{base} + \text{nucleoside}} \times 100$$

Only conversion rates that were linear with respect to time and amount of PyNP added, were considered for further analysis. This was usually the case if not more than 10% of the substrate was converted.

2′-Deoxy-2′-fluorouridine was purchased from TCI Deutschland (Eschborn, Germany) and 1-(2-deoxy-2-fluoro-β-D-arabinofuranosyl)uracil obtained from Metkinen Chemistry (Kuusisto, Finland). Other chemical reagents were purchased from Sigma–Aldrich.

2.6.1. Thermal stability

Enzyme preparations were diluted 1:100 in 50 mM potassium phosphate buffer (pH 7.0) yielding enzyme concentrations of about 46 μg ml^{-1}. These diluted enzyme solutions were aliquoted and incubated in 0.2 ml tubes in a thermocycler at the respective temperatures. After defined time intervals, tubes were withdrawn and the residual activity of the incubated enzyme solution was determined (at 60 °C for GtPyNP and at 80 °C for TtPyNP) and plotted over the reaction time. In order to determine the half life, the resulting curve was fitted (Sigma Plot) to the decay function:

$$v = v_0 \cdot e^{k_i \cdot t}$$

and subsequently the half life was calculated:

$$t_{1/2} = \ln 0.5 \cdot {k_i}^{-1}$$

2.6.2. Temperature optimum

The reaction mixture was pre-heated for 2 min at respective temperatures. The diluted enzyme solution was added and the

reaction was stopped after 3 min. 50 mM potassium phosphate buffer (pH 7.5) was used.

2.6.3. Kinetic parameters

Activity tests were performed in triplicates for at least 5 different substrate concentrations spanning 0.25–5 times of the Michaelis–Menton constant. The initial reaction rates were plotted over the substrate concentrations and fitted to the Michaelis–Menton function (Sigma Plot). From the resulting formula K_m and v_{max} were directly retrieved, and k_{cat} could be easily calculated. For details see [28].

2.6.4. Phosphorolysis of modified nucleosides

Reactions were performed in 1 mM pyrimidine nucleoside substrate solution containing 10 mM sodium phosphate buffer (pH 6.5) and an enzyme loading of ca. 0.1 mg ml^{-1} at either 60 °C or 80 °C.

2.6.5. HPLC analysis

The amount of pyrimidine nucleosides and corresponding bases was determined by following the absorption at 260 nm during HPLC analysis using a reversed phase C18 column (Gemini-Nx 5u, 150 × 4.60 mm, Phenomenex) with the following gradient: from 97% 20 mM ammonium acetate and 3% acetonitrile to 60% 20 mM ammonium acetate and 40% acetonitrile in 10 min. Under these conditions the following retention times were determined: uridine (3.2 min), uracil (2.4 min), thymidine (4.7 min), thymine (4.0 min), dUrd$^{2'F}$ (4.6 min), dUrd$_{2'F}$ (4.4 min), O^2,2′-anhydro-1-(β-D-arabinofuranosyl)uracil (2.3 min), 1-(β-D-arabinofuranosyl)uracil (3.8 min).

1-(β-D-Arabinofuranosyl)uracil was purchased from Sigma–Aldrich, O^2,2′-anhydro-1-(β-D-arabinofuranosyl)uracil was synthesized as described in [29].

3. Results and discussion

3.1. Sequence analysis and homology modeling

The proteins recombinantly expressed and characterized in this work are the pyrimidine nucleoside phosphorylases from *T. thermophilus* HB27 (GenBank accession number AAS81754.1) and from *G. thermoglucosidasius* 11955. The sequence of the latter corresponded to the PyNP sequence from *G. thermoglucosidasius* C56-YS93 (GenBank accession number ZP_06809030), with the exception of one amino acid. Since the corresponding deviation of the DNA sequence was suspected to be the result of the PCR performed for cloning, the respective codon was changed by site-directed mutagenesis to fit the data bank protein (Gln_{214} changed to Arg).

Three entries of solved crystal structures of PyNPs can be found in the protein database (www.pdb.org). Both target enzyme sequences were blasted against the amino acid sequences belonging to these pdb entries. GtPyNP aligned best with the PyNP from *G. stearothermophilus ATCC* 12980 (assigned here as GsPyNP, pdb entry 1BRW) with 78% sequence identity. TtPyNP aligned best with the PyNP from *T. thermophilus* HB8 (pdb entry 2DSJ), to which it is almost identical (approx. 98% sequence identity) but showed also a high degree of sequence identity (approx. 50%) to GsPyNP. The amino acid sequence alignment of GsPyNP, GtPyNP, TtPyNP and *E. coli* thymidine phosphorylase (EcTP) is shown in Fig. 1. Amino

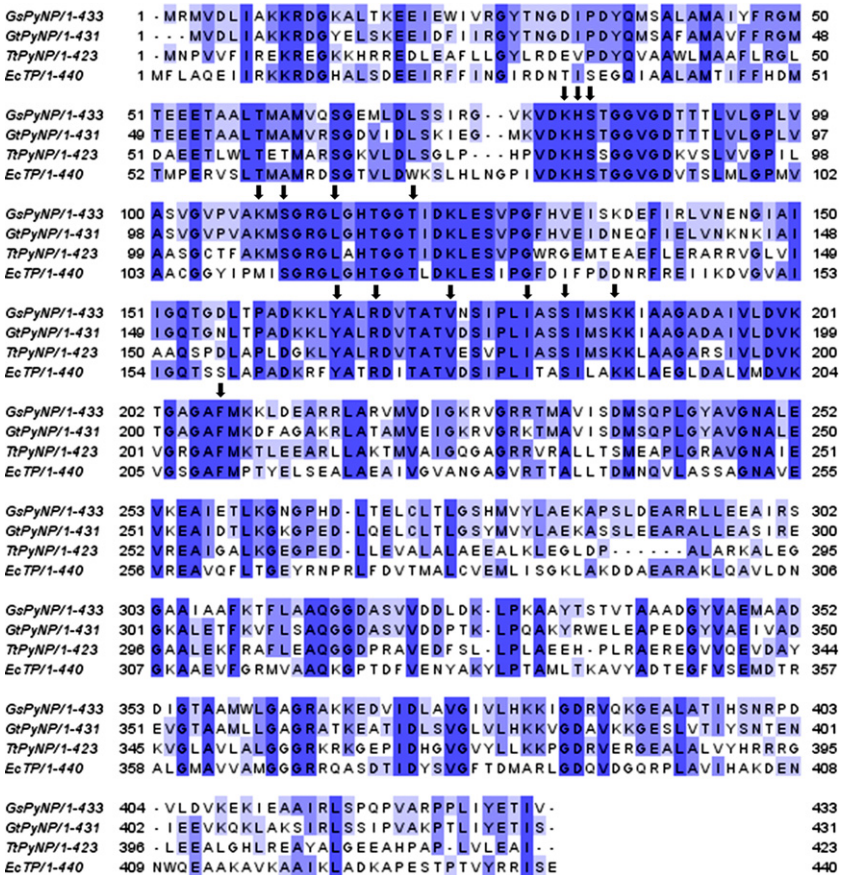

Fig. 1. 1Multiple sequence alignment of PyNP from *G. stearothermophilus* (GsPyNP), *G. thermoglucosidasius* (GtPyNP), *T. thermophilus* (TtPyNP) and TP from *E. coli* (EcTP). Shading represents the degree of sequence identity. Residues of the active site pocket are highlighted.

Fig. 2. 3D structure models. The superposition of GtPyNP (purple), TtPyNP (yellow) and GsPyNP (grey) 3D structures are shown. Structural models of GtPyNP and TtPyNP were built based on homology modeling using the structure of GsPyNP as template. (For interpretation of the references to color in this figure legend, the reader is referred to the web version of the article.)

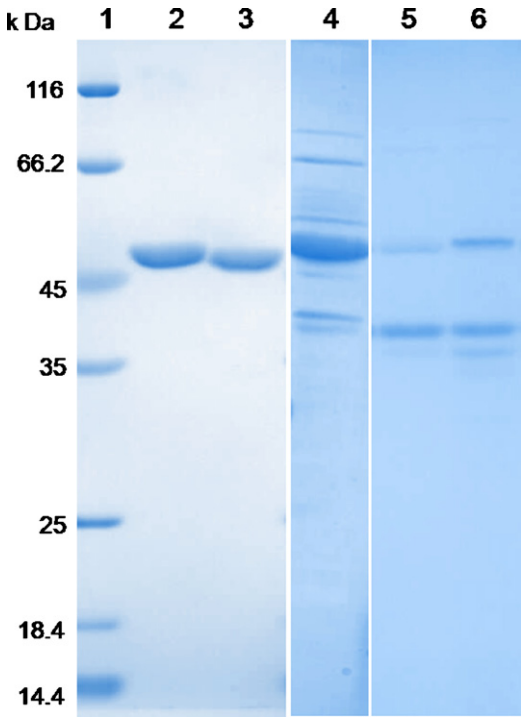

Fig. 3. SDS-PAGE of GtPyNP and TtPyNP samples. Recombinant expression of GtPyNP under standard conditions (37 °C, TB medium) was very efficient (4), but the expression of TtPyNP under the same conditions rather unsatisfactory (5). The expression level of TtPyNP could be significantly increased by using EnPresso medium that provides fed-batch like expression conditions (6). Purified GtPyNP (2) and TtPyNP (3) showed bands corresponding to the theoretically calculated molecular weight of the subunits (47.6 kDa and 46.9 kDa, respectively). Lane (1) represents the molecular weight marker.

acids that have been described to be involved in substrate binding or in the catalytic mechanism, respectively, are indicated [30,31].

The chain B of GsPyNP (pdb code 1BRW) was used as template to model both TtPyNP and GtPyNP. The structure of GsPyNP was elucidated in its closed conformation [30], uracil and the phosphate ion can be seen in the active site pocket. The structural fold of the models of GtPyNP and TtPyNP are almost identical to the template structure GsPyNP, which can be seen in the superposition of the secondary structure elements (Fig. 2).

3.2. Expression and purification

The desired sequences were expressed with an artificial N-terminal hexahistidine tag. In addition to a simple protein purification procedure this method offers the possibility to avoid expression problems associated with secondary structure formation of the 5′-end of mRNA, which is a critical issue, especially for genes derived from thermophiles [32]. Initially, the recombinant expression in *E. coli* of both GtPyNP and TtPyNP was performed under standard conditions (37 °C) in terrific broth (TB) medium. While the expression level of GtPyNP was satisfactory from the beginning (Fig. 3, lane 4), TtPyNP was expressed only very poorly (Fig. 3, lane 5). Hence, we tested also EnPresso medium for TtPyNP expression. This medium is based on an enzyme controlled substrate delivery and was reported to lead to higher cell densities and productivity per cell [33]. Indeed, the expression level of TtPyNP increased significantly (Fig. 3, lane 6) and the final cell density doubled (from $OD_{600} = 11$ to $OD_{600} = 22$). The volumetric yield obtained with this condition for TtPyNP expression was 0.06 mg ml^{-1}. Expression of GtPyNP in TB medium resulted in a volumetric yield of 0.17 mg ml^{-1}. Applied to SDS-PAGE gels, the purified proteins showed bands representing molecular weights that are consistent with the theoretically calculated values of the monomers (Fig. 3, lanes 2 and 3).

3.3. Thermal characteristics

The effect of temperature on the activity of the enzymes, as well as their thermal stability was investigated.

GtPyNP showed a temperature optimum of 60 °C, while the relative activity of TtPyNP increased with the reaction temperature, up to the highest temperature tested (99 °C, Fig. 4A). An apparent melting temperature of ≥102 °C and 103 °C was determined by circular dichroism and differential scanning calorimetry, respectively (Fig. 5). Hence, we assume that the temperature optimum of TtPyNP is in the range of 95–103 °C.

The stability half life of GtPyNP was estimated to be 1.6 h at 70 °C; while at 60 °C no significant loss of activity could be seen within 16 h of incubation. The stability half life of TtPyNP at 80 °C exceeds 23 h (Fig. 4B).

Compared to other reported enzymes with pyrimidine nucleoside phosphorylase activity, including UPs and TPs, the thermal stability and the temperature optimum of TtPyNP are extremely high (Table 1).

3.4. Kinetic parameters

Kinetic parameters describing the biocatalytical properties were determined at 60 °C for GtPyNP and at 80 °C for TtPyNP. The results are summarized in Table 2. The estimated K_m values of TtPyNP for the natural substrates uridine and thymidine are slightly lower than the K_m values determined by Hori et al. [1] for GsPyNP. In contrast to TtPyNP, GtPyNP is characterized by extremely low substrate affinities (high K_m values) towards both natural substrates.

The catalytic efficiency of an enzyme is best described by the ratio of k_{cat}/K_m [28]. These ratios are 15 times (substrate

Table 1
Thermal characteristics of reported PyNP, UP and TP.

Enzyme	Organism	Thermal stability ($t_{1/2}$)	Temp. optimum	Reference
TP	*E. coli*	<10 min (55 °C)	–	[34]
UP	*E. coli*	9.9 h (60 °C)	40 °C	[35]
PyNP	*G. thermoglucosidasius*	1.6 h (70 °C)	60 °C	This study
$UP_{engineered}$	*E. coli*	3.3 h (70 °C)	60 °C	[35]
UP	*Enterobacter aerogenes*	1 week (60 °C)	65 °C	[36]
PyNP	*G. stearothermophilus*	25 min (70 °C)	70 °C	[1,2]
UP	*Erwinia carotovora*	–	70 °C	[37]
PyNP	*T. thermophilus*	>24 h (80 °C)	>95 °C	This study

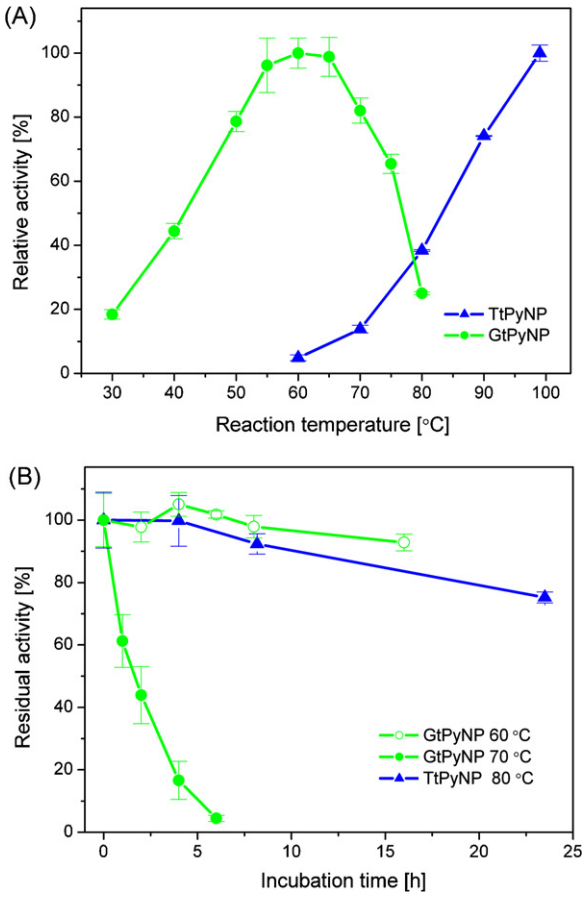

Fig. 4. Thermal characteristics. Relative activity of GtPyNP and TtPyNP over the reaction temperature (A), where the highest reaction rate determined was set to 100% for each enzyme. Thermostability (B) was investigated by incubating protein samples for defined time intervals and subsequently determining the residual activity, where the activity of enzyme samples that were not thermo-treated was set to 100%.

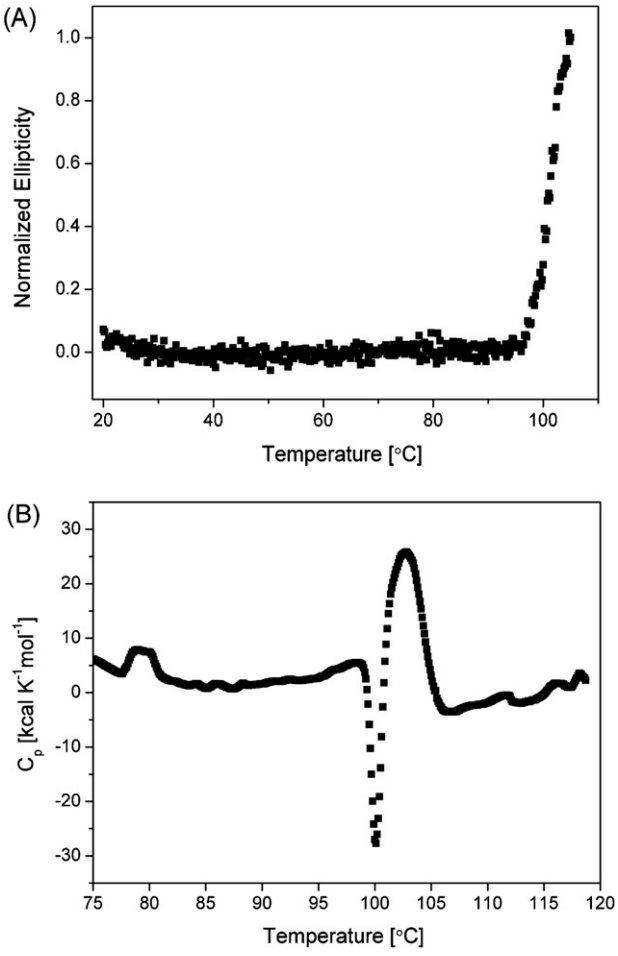

Fig. 5. Thermal unfolding of TtPyNP. Thermal unfolding trace monitored by loss of the far-UV circular dichroism signal at 220 nm provided an apparent melting temperature of at least 102 °C (A). The apparent melting temperature determined by differential scanning calorimetry (B) was 103 °C.

uridine) and 25 times (substrate thymidine) higher for TtPyNP than for GtPyNP. The k_{cat}/K_m ratio is also a measure to compare an enzyme's specificity towards different substrates [28]. The results of the present study show that both enzymes are more specific for uridine than for thymidine, but the difference in specificity is more pronounced for GtPyNP: the k_{cat}/K_m ratio is 2 fold higher for uridine than for thymidine. In contrast, the k_{cat}/K_m ratio of TtPyNP is only 1.23 fold higher for uridine vs that of thymidine.

Table 2
Kinetic parameters of reported PyNP in comparison to *E. coli* enzymes TP and UP.

Enzyme	K_m (μM)		k_{cat} (s^{-1})		k_{cat}/K_m (s^{-1} μM^{-1})		React. conditions	Reference
	Uridine	Thymidine	Uridine	Thymidine	Uridine	Thymidine		
GtPyNP	2342	1282	275	83	0.12	0.06	60 °C, pH 7.0	This study
TtPyNP	145	435	279	679	1.92	1.56	80 °C, pH 7.0	This study
GsPyNP	190	460	–	–	–	–	60 °C, pH 7.0	[1]
EcTP	60	300	$<1 \times 10^{-4}$	198	$<1.7 \times 10^{-6}$	0.66	25 °C, pH 6.5	[38,39]
EcUP	80	270	98	5	1.22	0.02	25 °C, pH 7.5	[38,40]

The estimation errors of the K_m and k_{cat} values determined in this study were not higher than 10%. (–) Data not indicated.

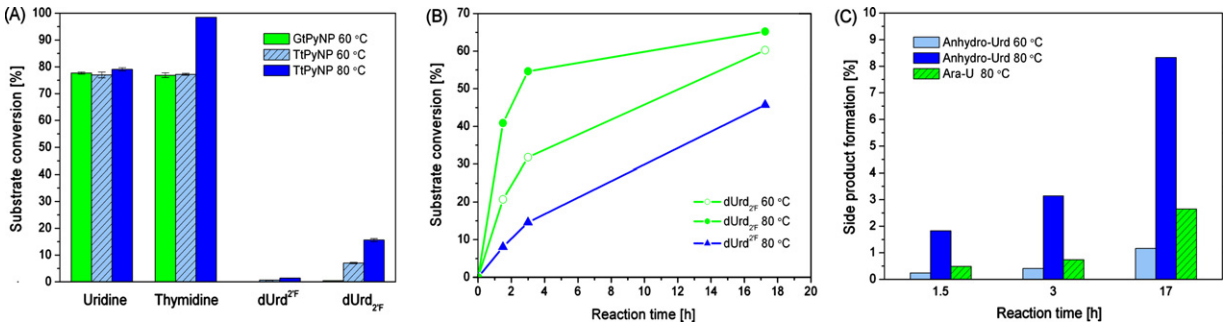

Fig. 6. Phosphorolysis of natural and modified pyrimidine nucleosides. (A) The percentage of natural and 2′-fluorosubstituted pyrimidine nucleosides that were phosphorolytically cleaved by TtPyNP or GtPyNP after 30 min, (B) percentage of 2′-fluorosubstituted pyrimidine nucleosides phosphorolytically cleaved by TtPyNP after prolonged reaction times at indicated temperatures and (C) percentage of $dUrd_{2'F}$ molecules that reacted to anhydro-Urd and ara-U during the TtPyNP catalyzed phosphorolytic cleavage reaction in dependence of reaction time and temperature. The ara-U formation at 60 °C could not be accurately determined but was estimated not to be higher than 0.4%.

In synthetic applications, where high substrate concentrations are used ($c_s \gg K_m$) the k_{cat} value may be the most appropriate parameter describing the efficiency of the biocatalyst. The turnover numbers (k_{cat}) of GtPyNP and TtPyNP are in similar range, with uridine as substrate. By contrast, the turnover numbers for thymidine differ significantly, in favor of thymidine phosphorolysis by TtPyNP. The k_{cat} value of TtPyNP for thymidine is also unusually high in comparison to alternative enzymes that are used for the phosphorolysis of pyrimidine nucleosides, e.g. EcUP and EcTP (Table 2).

3.5. Phosphorolysis of 2′-fluoro substituted pyrimidine nucleosides

Of particular interest is the potential of both thermostable PyNPs as biocatalysts in the synthesis of modified nucleosides. With this aim in view, the phosphorolysis of natural pyrimidine nucleoside substrates (thymidine and uridine) and their sugar modified analogues, *viz.*, 2′-deoxy-2′-fluorouridine ($dUrd_{2'F}$) and 1-(2-deoxy-2-fluoro-β-D-arabinofuranosyl)uracil ($dUrd^{2'F}$), were investigated. These substrates can be used as pentofuranosyl donors in enzymatic transglycosylations aiming at the synthesis of pharmaceutically valuable 2′-fluorosubstituted purine nucleosides. With this strategy $dUrd_{2'F}$ served as a substrate for the enzymatic synthesis of 2′-deoxy-2′-fluoroguanosine using the whole *E. coli* cells as a biocatalyst [41] and a multitude of other purine 2′-deoxy-2′-fluororibosides with antiviral activity using a combination of EcTP and EcPNP as a biocatalyst [42].

However, $dUrd_{2'F}$ and $dUrd^{2'F}$ are very poor substrates in phosphorolysis reactions. This is presumably a result of increased strength of the glycosyl bond as it follows from the crystallographic data for the N1–C1′ bond length of uridine (aver. value 1.490 Å [43]) and its 2′-deoxyfluoro analogues (1.454 Å [44] and 1.460 Å [45], respectively). Moreover, introduction of a fluorine atom into pentofuranose ring of nucleosides results in dramatic changes of the conformation of such analogues precluding the formation of the productive substrate-catalytic center complex (for more detailed discussion, see [11]).

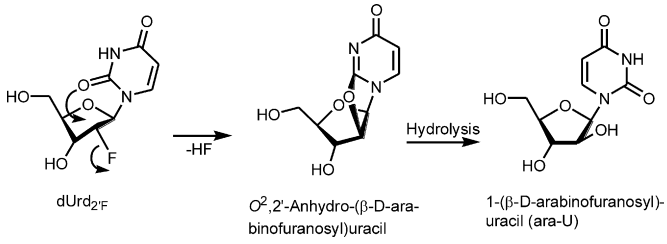

Scheme 3.

Indeed, it was reported that (i) $dUrd_{2'F}$ showed no detectable substrate activity towards EcUP, (ii) EcTP catalyzed the phosphorolysis of $dUrd_{2'F}$ but at an extremely low rate, and (iii) the enzymatic cleavage of the glycosidic bond of $dUrd^{2'F}$ equally afforded a high amount of enzyme and prolonged reaction time (6 days) [42,46].

In this study we have investigated the phosphorolysis of these challenging substrates by GtPyNP and TtPyNP (Fig. 6). Our results indicate that TtPyNP might be a good alternative to the use of *E. coli* enzymes, but the use of GtPyNP is apparently not suitable for the applications discussed above: no activity towards $dUrd^{2'F}$ and only poor activity towards $dUrd_{2'F}$ (0.44% substrate conversion) was detected with GtPyNP as biocatalyst after 30 min reaction time.

By contrast, the TtPyNP catalyzed reaction under the same conditions resulted in the phosphorolytic cleavage of 0.65% of $dUrd^{2'F}$ and 7.0% of $dUrd_{2'F}$. Since the optimal reaction temperature of TtPyNP is significantly higher than 60 °C (see Section 3.3), we repeated the same reaction also at 80 °C. Now, the TtPyNP catalyzed reaction resulted in 1.4% phosphorolyzed $dUrd^{2'F}$ and 15.6% of $dUrd_{2'F}$. However, under these conditions the formation of two new peaks were observed by HPLC analysis of the reaction mixture that contained $dUrd_{2'F}$. The retention times coincide with those of authentic samples of O^2,2′-anhydro-1-(β-D-arabinofuranosyl)uracil (anhydro-Urd) (2.3 min) and 1-(β-D-arabinofuranosyl)uracil (ara-U) (3.8 min). Hence, the formation of anhydro-Urd resulting from HF release from the $dUrd_{2'F}$ molecule and the subsequent hydrolysis of anhydro-Urd resulting in ara-U appear to be a reasonable explanation (Scheme 3). Phosphorolysis of both 2′-fluorosubstituted pyrimidine nucleosides catalyzed by TtPyNP was also monitored over prolonged reaction times (Fig. 6B). The results show that the conversion of $dUrd^{2'F}$ at 80 °C could be increased to 46% after 17 h; side-product formation was not observed. The final amount of phosphorolyzed $dUrd_{2'F}$ after 17 h at 80 °C (65%) was in similar range as the amount obtained at 60° (60%). By contrast, side product formation, as discussed above, at 80 °C was significantly higher than at 60 °C (Fig. 6C). After 17 h 8.3% of $dUrd_{2'F}$ reacted to anhydro-Urd at 80 °C, whereas only 1.2% of $dUrd_{2'F}$ reacted to anhydro-Urd at 60 °C.

4. Conclusion

PyNPs isolated from thermophilic microorganisms are promising biocatalysts for the efficient synthesis of modified nucleosides [18]. Up to now, the biocatalytic characterization of PyNPs from thermophilic microbes was restricted to PyNPs from *G. stearothermophilus* strains [1,2,6]. We have studied here the biocatalytical properties of two additional thermostable PyNP, originating from *G. thermoglucosidasius* and *T. thermophilus.*

Our results indicate that both enzymes show excellent biocatalytical properties for applications with natural pyrimidine nucleosides as substrates (thymidine, uridine) and a reaction temperature of 60 °C. In addition, the unusually high thermal stability of TtPyNP makes this biocatalyst also suitable for reactions requiring an even higher reaction temperature of 80 °C.

We have further tested both thermostable PyNPs towards their ability to phosphorolyze 2′-fluorosubstituted pyrimidine nucleosides that have been shown to be very poor substrates in phosphorolysis reactions employing EcUP or EcTP as biocatalyst [42,46]. Our results reveal striking differences of the substrate specificities of GtPyNP and TtPyNP, in favor of the latter. These findings make TtPyNP a candidate as powerful biocatalyst in the transglycosylation reactions aiming at the synthesis of 2′-fluoro substituted purine nucleosides. Expression of appropriate PNPs and their use in synthetic applications are ongoing.

Acknowledgments

This work is part of the Cluster of Excellence "Unifying Concepts in Catalysis" coordinated by the Technische Universität Berlin. Financial support by the Deutsche Forschungsgemeinschaft (DFG) within the framework of the German Initiative for Excellence is gratefully acknowledged (EXC 314). We would like to thank Prof. Reinhard Sterner (Institute of Biophysics and Physical Biochemistry, University of Regensburg) for his support and providing us the facilities for protein analytical measurements. 1-(2-Deoxy-2-fluoro-β-D-arabinofuranosyl)uracil was kindly provided by Prof. Alex Azhayev (Metkinen Chemistry). We further thank Prof. Xiaoda Yang (School of Pharmaceutical Sciences, Peking University Health Science Centre), Dr. Andy Maraite and Prof. Marion Ansorge-Schumacher (Technische Universität Berlin) for fruitful discussions.

References

[1] N. Hori, M. Watanabe, Y. Yamazaki, Y. Mikami, Agric. Biol. Chem. 54 (1990) 763–768.
[2] T. Hamamoto, T. Noguchi, Y. Midorikawa, Biosci. Biotechnol. Biochem. 60 (1996) 1179–1180.
[3] M.J. Pugmire, S.E. Ealick, J. Biochem. 361 (2002) 1–25.
[4] T. Furukawa, A. Yoshimura, T. Sumizawa, M. Haraguchi, S. Akiyama, K. Fukui, M. Ishizawa, Y. Yamada, Nature 356 (1992) 668.
[5] S. Akiyama, T. Furukawa, T. Sumizawa, Y. Takebayashi, Y. Nakajima, S. Shimaoka, M. Haraguchi, Cancer Sci. 95 (2004) 851–857.
[6] P.P. Saunders, B.A. Wilson, G.F. Saunders, J. Biol. Chem. 244 (1969) 3691–3697.
[7] M.G. Vander Heiden, Nat. Rev. Drug Discov. 10 (2011) 671–684.
[8] E. De Clercq, Annu. Rev. Pharmacol. 51 (2011) 1–24.
[9] A.J. Berdis, Biochemistry 47 (2008) 8253–8260.
[10] P. Herdewijn, Modified Nucleosides in Biochemistry, Biotechnology and Medicine, Wiley-VCH, Weinheim, 2008.
[11] I.A. Mikhailopulo, A.I. Miroshnikov, Mendeleev Commun. 21 (2011) 57–68.
[12] N. Hori, M. Watanabe, Y. Yamazaki, Y. Mikami, Agric. Biol. Chem. 53 (1989) 2205–2210.
[13] A. Bzowska, E. Kulikowska, D. Shugar, Pharmacol. Ther. 88 (2000) 349–425.
[14] G. Cacciapuoti, S. Gorassini, M.F. Mazzeo, R.A. Siciliano, V. Carbone, V. Zappia, M. Porcelli, FEBS J. 274 (2007) 2482–2495.
[15] D. Visser, F. Hennessy, K. Rashamuse, M. Louw, D. Brady, Extremophiles 14 (2010) 185–192.
[16] X.F. Gao, X.R. Huang, C.C. Sun, J. Struct. Biol. 154 (2006) 20–26.
[17] K. Shimizu, N. Kunishima, Acta Crystallogr. F 63 (2007) 308–310.
[18] S.A. Taran, K.N. Verevkina, S.A. Feofanov, A.I. Miroshnikov, Russ. J. Bioorg. Chem. 35 (2009) 739–745.
[19] T. Schwab, R. Sterner, Chembiochem 12 (2011) 1581–1588.
[20] D. Moore, D. Dowhan, in: F.M. Ausubel, et al. (Eds.), Purification and Concentration of DNA from Aqueous Solutions, John Wiley & Sons, Houston, 2002, Unit 2.1A.
[21] J. Šiurkus, J. Panula-Perälä, U. Horn, M. Kraft, R. Rimšeliene, P. Neubauer, Microb. Cell Fact. 9 (2010) 35.
[22] K. Gerdes, Biotechnology 6 (1988) 1402–1405.
[23] S.F. Altschul, W. Gish, W. Miller, E.W. Myers, D.J. Lipman, J. Mol. Biol. 215 (1990) 403–410.
[24] M.A. Larkin, G. Blackshields, N.P. Brown, R. Chenna, P.A. McGettigan, H. McWilliam, F. Valentin, I.M. Wallace, A. Wilm, R. Lopez, J.D. Thompson, T.J. Gibson, D.G. Higgins, Bioinformatics 23 (2007) 2947–2948.
[25] L. Bordoli, F. Kiefer, K. Arnold, P. Benkert, J. Battey, T. Schwede, Nat. Protoc. 4 (2009) 1–13.
[26] S. McNicholas, E. Potterton, K.S. Wilson, M.E.M. Noble, Acta Crystallogr. D 67 (2011) 386–394.
[27] J. Sambrook, D.W. Russell, Molecular Cloning: A Laboratory Manual, 3rd ed., Cold Spring Harbor Laboratory Press, New York, 2001.
[28] R.A. Copeland, ENZYMES a Practical Introduction to Structure, Mechanism, and Data Analysis, 2nd ed, Wiley-VCH, New York, 2000.
[29] A.A. Akhrem, G.V. Zaitseva, I.A. Mikhailopulo, A.F. Abramov, J. Carbohydr. Nucl. 4 (1977) 43–63.
[30] M.J. Pugmire, S.E. Ealick, Structure 6 (1998) 1467–1479.
[31] J. Mendieta, S. Martin-Santamaria, E.M. Priego, J. Balzarini, M.J. Camarasa, M.J. Perez-Perez, F. Gago, Biochemistry 43 (2004) 405–414.
[32] K. Szeker, O. Niemitalo, M.G. Casteleijn, A.H. Juffer, P. Neubauer, J. Biotechnol. 156 (2010) 268–274.
[33] K. Ukkonen, A. Vasala, H. Ojamo, P. Neubauer, Microb. Cell Fact. 10 (2011) 107.
[34] T.A. Krenitsky, J.V. Tuttle, Biochim. Biophys. Acta 703 (1982) 247–249.
[35] D.F. Visser, F. Hennessy, J. Rashamuse, B. Pletschke, D. Brady, J. Mol. Catal. B: Enzym. 68 (2011) 279–285.
[36] T. Utagawa, H. Morisawa, Y. Shigeru, A. Yamazaki, F. Yoshinaga, Y. Hirose, Agric. Biol. Chem. 49 (1985) 3239–3246.
[37] H. Shirae, K. Yokozeki, Agric. Biol. Chem. 55 (1991) 1849–1857.
[38] N.G. Panova, E.V. Shcheveleva, K.S. Alekseev, V.G. Mukhortov, A.N. Zuev, S.N. Mikhailov, R.S. Esipov, D.V. Chuvikovskii, A.I. Miroshnikov, Mol. Biol. (Mosk) 38 (2004) 907–913.
[39] N.G. Panova, C.S. Alexeev, A.S. Kuzmichov, E.V. Shcheveleva, S.A. Gavryushov, K.M. Polyakov, A.M. Kritzyn, S.N. Mikhailov, R.S. Esipov, A.I. Miroshnikov, Biochemistry (Moscow) 72 (2007) 21–28.
[40] C.S. Alexeev, N.G. Panova, K.M. Polyakov, S.N. Mikhailov, Abstracts of XIX International Round Table on Nucleosides, Nucleotides and Nucleic Acids IRT 2010, 2010, p. 94.
[41] G.V. Zaitseva, A.I. Zinchenko, V.N. Barai, N.I. Pavlova, E.I. Boreko, I.A. Mikhailopulo, Nucleosides Nucleotides 18 (1999) 687–688.
[42] J.V. Tuttle, M. Tisdale, T.A. Krenitsky, J. Med. Chem. 36 (1993) 119–125.
[43] E.A. Green, R.D. Rosenstein, R. Shiono, D.J. Abraham, B.L. Trus, R.E. Marsh, Acta Crystallogr. B 31 (1975) 102–107.
[44] C. Marck, B. Lesyng, W. Saenger, J. Mol. Struct. 82 (1982) 77–94.
[45] A. Hempel, N. Camerman, J. Grierson, D. Mastropaolo, A. Camerman, Acta Crystallogr. C 55 (1999) 632–633.
[46] J.V. Tuttle, T.A. Krenitsky, European Patent Publication EP 0285432 B1 (1992).